12-14-2011

Long-Term Systemic Myostatin Inhibition via Liver-Targeted Gene Transfer in Golden Retriever Muscular Dystrophy

Lawrence T. Bish
University of Pennsylvania, bish@mail.med.upenn.edu

Margaret M. Sleeper
University of Pennsylvania, sleeper@vet.upenn.edu

Sean C. Forbes

Kevin J. Morine

Caryn A. Reynolds
University of Pennsylvania

See next page for additional authors

Recommended Citation

Bish, L. T., Sleeper, M. M., Forbes, S. C., Morine, K. J., Reynolds, C. A., Singletary, G. E., Trafny, D., Pham, J., Bogan, J., Kornegay, J. N., Vandenborne, K., Walter, G. A., & Sweeney, H. L. (2011). Long-Term Systemic Myostatin Inhibition via Liver-Targeted Gene Transfer in Golden Retriever Muscular Dystrophy. *Human Gene Therapy, 22* (12), 1499-1509. http://dx.doi.org/10.1089/hum.2011.102

Long-Term Systemic Myostatin Inhibition via Liver-Targeted Gene Transfer in Golden Retriever Muscular Dystrophy

Abstract

Duchenne muscular dystrophy (DMD) is a lethal, X-linked recessive disease affecting 1 in 3,500 newborn boys for which there is no effective treatment or cure. One novel strategy that has therapeutic potential for DMD is inhibition of myostatin, a negative regulator of skeletal muscle mass that may also promote fibrosis. Therefore, our goal in this study was to evaluate systemic myostatin inhibition in the golden retriever model of DMD (GRMD). GRMD canines underwent liver-directed gene transfer of a self-complementary adeno-associated virus type 8 vector designed to express a secreted dominant-negative myostatin peptide (n =4) and were compared with age-matched, untreated GRMD controls (n =3). Dogs were followed with serial magnetic resonance imaging (MRI) for 13 months to assess cross-sectional area and volume of skeletal muscle, then euthanized so that tissue could be harvested for morphological and histological analysis. We found that systemic myostatin inhibition resulted in increased muscle mass in GRMD dogs as assessed by MRI and confirmed at tissue harvest. We also found that hypertrophy of type IIA fibers was largely responsible for the increased muscle mass and that reductions in serum creatine kinase and muscle fibrosis were associated with long-term myostatin inhibition in GRMD. This is the first report describing the effects of long-term, systemic myostatin inhibition in a large-animal model of DMD, and we believe that the simple and effective nature of our liver-directed gene-transfer strategy makes it an ideal candidate for evaluation as a novel therapeutic approach for DMD patients.

Disciplines

Comparative and Laboratory Animal Medicine | Congenital, Hereditary, and Neonatal Diseases and Abnormalities | Diseases | Medicine and Health Sciences | Musculoskeletal Diseases | Veterinary Medicine

Author(s)

Lawrence T. Bish, Margaret M. Sleeper, Sean C. Forbes, Kevin J. Morine, Caryn A. Reynolds, Gretchen E. Singletary, Dennis Trafny, Jennifer Pham, Janet Bogan, Joe N. Kornegay, Krista Vandenborne, Glenn A. Walter, and H. Lee Sweeney

HUMAN GENE THERAPY 22:1499–1509 (December 2011)

DOI: 10.1089/hum.2011.102

Long-Term Systemic Myostatin Inhibition via Liver-Targeted Gene Transfer in Golden Retriever Muscular Dystrophy

Lawrence T. Bish,[1,*] Meg M. Sleeper,[2,*] Sean C. Forbes,[3] Kevin J. Morine,[1] Caryn Reynolds,[2] Gretchen E. Singletary,[2] Dennis Trafny,[2] Jennifer Pham,[1] Janet Bogan,[4] Joe N. Kornegay,[4] Krista Vandenborne,[3] Glenn A. Walter,[5] and H. Lee Sweeney[1]

Abstract

Duchenne muscular dystrophy (DMD) is a lethal, X-linked recessive disease affecting 1 in 3,500 newborn boys for which there is no effective treatment or cure. One novel strategy that has therapeutic potential for DMD is inhibition of myostatin, a negative regulator of skeletal muscle mass that may also promote fibrosis. Therefore, our goal in this study was to evaluate systemic myostatin inhibition in the golden retriever model of DMD (GRMD). GRMD canines underwent liver-directed gene transfer of a self-complementary adeno-associated virus type 8 vector designed to express a secreted dominant-negative myostatin peptide ($n = 4$) and were compared with age-matched, untreated GRMD controls ($n = 3$). Dogs were followed with serial magnetic resonance imaging (MRI) for 13 months to assess cross-sectional area and volume of skeletal muscle, then euthanized so that tissue could be harvested for morphological and histological analysis. We found that systemic myostatin inhibition resulted in increased muscle mass in GRMD dogs as assessed by MRI and confirmed at tissue harvest. We also found that hypertrophy of type IIA fibers was largely responsible for the increased muscle mass and that reductions in serum creatine kinase and muscle fibrosis were associated with long-term myostatin inhibition in GRMD. This is the first report describing the effects of long-term, systemic myostatin inhibition in a large-animal model of DMD, and we believe that the simple and effective nature of our liver-directed gene-transfer strategy makes it an ideal candidate for evaluation as a novel therapeutic approach for DMD patients.

Introduction

Duchenne muscular dystrophy (DMD) is a lethal, X-linked recessive disease affecting one in 3,500 newborn boys that results from a mutation in the dystrophin gene (Emery, 2002). Thousands of mutations in the 79-exon dystrophin gene have been reported, with the most severe cases being associated with disruption of the reading frame and loss of functional dystrophin production (Aartsma-Rus *et al.*, 2006). Boys typically present with symptoms of muscle weakness by age five, become wheelchair-bound by early to mid teens, and die from respiratory failure or cardiomyopathy in their late teens to early twenties (Muntoni *et al.*, 2003; Tyler, 2003; Wang *et al.*, 2009). Patients with dystrophin mutations that maintain the reading frame and produce truncated but partially functional dystrophin exhibit the milder phenotype of Becker muscular dystrophy (Aartsma-Rus *et al.*, 2006). Unfortunately, no effective therapy or cure exists for DMD, and novel therapeutic strategies are in need of development.

Gene therapy is one approach that has potential as a novel treatment for DMD (Wang *et al.*, 2009). The majority of gene-therapy investigations have focused on strategies aimed at restoring dystrophin expression or increasing muscle mass and have been performed in either the *mdx* mouse (Sicinski *et al.*, 1989) or canine X-linked muscular dystrophy (Valentine *et al.*, 1988; Sharp *et al.*, 1992) models of DMD. Restoration of dystrophin expression has been accomplished by gene transfer of mini- and microdystrophin constructs in dystrophic mice (Harper *et al.*, 2002; Gregorevic *et al.*, 2004; Liu *et al.*, 2005), dogs (Wang *et al.*, 2007; Kornegay *et al.*, 2010), and humans (Miyagoe-Suzuki and Takeda, 2010), as well as by induction of exon skipping in dystrophic mice (Goyenvalle

[1]Department of Physiology, University of Pennsylvania School of Medicine, Philadelphia, PA 19104.
[2]Section of Cardiology, Department of Clinical Studies, Veterinary Hospital of the University of Pennsylvania, Philadelphia, PA 19104.
[3]Department of Physical Therapy, University of Florida, Gainesville, FL 32610.
[4]Departments of Pathology and Laboratory Medicine, Neurology, and the Gene Therapy Center, University of North Carolina–Chapel Hill, Chapel Hill, NC 27514.
[5]Department of Physiology and Functional Genomics, University of Florida, Gainesville, FL 32610.
*These two authors have contributed equally to this article.

et al., 2004; Denti *et al.*, 2006, 2008), dogs (Yokota *et al.*, 2009), and humans (Miyagoe-Suzuki and Takeda, 2010; Moulton and Moulton, 2010; Partridge, 2010). Proof-of-principle studies demonstrating successful gene transfer of microdystrophin (Rodino-Klapac *et al.*, 2010) and successful induction of exon skipping (Moulton and Moulton, 2010) have also been performed in healthy nonhuman primates (NHPs).

A second gene therapy–based strategy currently under investigation for the treatment of DMD is aimed at targeting the myostatin pathway to increase muscle mass and potentially decrease fibrosis and improve regeneration. Myostatin, a member of the transforming growth factor-β (TGF-β) family of proteins, is a negative regulator of skeletal muscle mass (McPherron *et al.*, 1997; Lee, 2004). Indeed, loss-of-function mutations leading to increased muscle mass have been described in several species (Lee, 2007b), including humans (Schuelke *et al.*, 2004), and investigators using gene transfer approaches have demonstrated that inhibition of myostatin can increase muscle mass and attenuate the dystrophic phenotype in *mdx* mice (Qiao *et al.*, 2008; Morine *et al.*, 2010a,b). Pharmacological and/or genetic targeting of the myostatin pathway has also been evaluated in dystrophic mice (Bogdanovich *et al.*, 2002, 2005, 2008; Wagner *et al.*, 2002; Pistilli *et al.*, 2011); however, the one human trial targeting a number of muscular dystrophies, including DMD, with an inhibitory myostatin antibody was not conclusive (Wagner *et al.*, 2008). Although proof-of-principle experiments in canines (Qiao *et al.*, 2009) and NHPs (Kota *et al.*, 2009) have demonstrated increased skeletal muscle mass following gene transfer of myostatin inhibitors, evaluation of myostatin inhibition in large-animal models of DMD has not yet been performed.

Therefore, our goal in this study was to evaluate systemic myostatin inhibition in the golden retriever model of DMD (GRMD). GRMD canines underwent liver-directed gene transfer of a self-complementary adeno-associated virus (AAV) type 8 (scAAV8) vector designed to express a secreted dominant-negative myostatin (dnMSTAT) peptide, a strategy that we previously evaluated in the *mdx* mouse (Morine *et al.*, 2010a). Dogs were followed for 13 months following gene transfer. We found that systemic myostatin inhibition resulted in increased muscle mass in GRMD canines as assessed by magnetic resonance imaging (MRI) and confirmed at tissue harvest. We also found that hypertrophy of type IIA fibers was largely responsible for the increased muscle mass and that reductions in serum creatine kinase (CK) and muscle fibrosis were associated with long-term myostatin inhibition in GRMD.

Materials and Methods

Vector design and production

scAAV8 vectors were produced according to the previously described pseudotyping protocol by the Vector Core of the Children's Hospital of Philadelphia (Herzog *et al.*, 1999). In brief, recombinant AAV genomes containing AAV2 inverted terminal repeats (ITRs) were packaged by triple transfection of 293 cells with a *cis*-plasmid containing the enhanced green fluorescent protein (EGFP) transgene, an adenovirus helper plasmid, and a chimeric *trans*-plasmid containing the AAV2 rep gene fused to the capsid gene of the AAV6. Self-complementary vectors contained a mutation in the termination sequence of the 5′ ITR to allow synthesis and encapsidation of a dimeric inverted repeat of the transgene cassette (McCarty *et al.*, 2001).

The scAAV8-TBG-dnMSTAT construct was designed to express the secreted canine myostatin Belgian Blue inhibitory peptide (Kambadur *et al.*, 1997) containing a D76A mutation that confers protease resistance (Wolfman *et al.*, 2003) under control of the liver-specific thryroid-hormone binding globulin (TBG) promoter (Bell *et al.*, 2011).

Animal use and vector delivery protocol

All animals were handled in compliance with National Institutes of Health and institutional guidelines that were approved by the Institutional Animal Care and Use Committee of the University of Pennsylvania. A total of nine canines were used in this study. At the time of treatment, dogs were 9–10 months old and weighed 14–19 kg. The scAAV8-TBG-dnMSTAT vector was tested in two normal canines prior to its use in GRMD canines. One normal canine received 10^{12} genome copies (gc)/kg vector via hepatic artery infusion as previously described (Bell *et al.*, 2011), and one normal canine received 10^{12} gc/kg vector via peripheral intravenous (IV) infusion (cephalic vein). The remaining dogs used in the study were GRMD canines, which received either 1.7×10^{12} gc/kg vector ($n=4$) via IV infusion or no treatment ($n=3$). Euthanasia occurred 13 months post infusion, at $\sim$23 months of age. GRMD canines were produced in a colony at the University of North Carolina at Chapel Hill and were cared for according to principles outlined in the National Institutes of Health Guide for the Care and Use of Laboratory Animals. The phenotype was initially determined based on elevation of serum creatine kinase and confirmed by PCR.

All canines used in this study were screened for the presence of preexisting neutralizing antibodies (NAbs) against AAV8. The AAV8 NAb titer for all canines was $<$1:20, which was the lower limit of detection in this assay. Titer was determined by incubating Huh7 cells with serial dilutions of canine serum and AAV-CMV-EGFP of the serotype in question and observing the dilution at which the number of GFP-positive cells was reduced by 50% compared with control wells.

RT-PCR analysis

Tissue collected for RT-PCR analysis was snap-frozen in liquid nitrogen and processed as described previously (Morine *et al.*, 2010a). Samples were crushed on a mortar and pestle cooled by dry ice, and total RNA was isolated from muscle homogenates by RNA TRIzol extraction (Invitrogen, Carlsbad, CA). One hundred fifty nanograms of RNA from each sample was subjected to single-strand reverse transcription, and the resulting cDNA was used in a PCR reaction with Taq polymerase (Applied Biosystems, Foster City, CA). The primers for dnMSTAT were as follows: forward 5′ GTT-TAG-CTC-TAA-AAT-ACA-ATA-TAA-TA 3′ and reverse 5′ AAC-TTG-TTT-ATT-GCA-GCT-TAT-AAT-G 3′. These primers were located within the transgene and SV40 poly(A) tail, respectively, to detect vector sequence specifically. Vector plasmid was used as a positive control for these primers. The primers for glyceraldehyde-3-phosphate dehydrogenase (GAPDH) were as follows: forward 5′ ATG-GTG-AAG-GTC-GGA-GTC-AAC-GGA-T 3′ and reverse 5′ GAA-GAT-GGA-GAT-GGA-CTT-CCC-GTT-G 3′. The resulting PCR reactions were run on a 1.5% agarose gel with ethidium bromide and visualized under ultraviolet light.

Western blot analysis

Cardiac biopsies obtained for western blotting were snap-frozen in liquid nitrogen. Specimens were pulverized, homogenized in 10 volumes of triple-detergent lysis buffer [50 m*M* Tris, pH 8.0, 0.1% sodium dodecyl sulfate (SDS), 1.0% Triton X-100, 0.5% deoxycorticosterone, 5 m*M* EDTA, 50 m*M* dithiothreitol (DTT), 0.4 tablet/10 ml Complete Protease Inhibitor (Roche, Indianapolis, IN)], and centrifuged at 13,000 rpm for 5 min. Protein concentration of the supernatant was then determined using the Bio-Rad Protein Assay (Bio-Rad, Hercules, CA). Fifty micrograms of each sample was electrophoresed on a 20% SDS-polyacrylamide gel (Lonza, Rockland, ME) following the addition of 2× sample loading buffer (130 m*M* Tris, pH 8.0, 20% glycerol, 4.6% SDS, 2% DTT, 0.02% bromophenol blue) and 5 min of denaturation at 100°C. Proteins were then transferred to Immobilon-P (Millipore, Bedford, MA) using the iBlot transfer apparatus (Invitrogen). The membrane was subsequently blocked with 5% nonfat dry milk in Tris-buffered saline containing 0.05% Tween 20. Immunoblotting was performed to detect myostatin N-terminus (1:1,000; R&D Systems, Minneapolis, MN). Detection was performed using the SuperSignal West Pico Chemiluminescent Substrate Kit (Pierce, Rockford, IL).

Muscle morphology and histology

The tibialis cranialis (TC), extensor digitorum longus (EDL), gastrocnemius, and flexor digitorum superficialis (FDS) muscles were explanted from the canine and weighed. Muscles were subsequently embedded in Optimal Cutting Temperature compound (Sakura Finetek, Torrance, CA) and frozen in liquid nitrogen–cooled isopentane. Ten-micrometer sections were cut, and the resulting slides were stored at −20°C.

Immunohistochemistry was used to determine the fiber sizes, fiber number, and myosin heavy-chain (MHC) composition of examined muscles as described previously (Barton *et al.*, 2002). Sections were blocked in 5% bovine serum albumin (BSA) in phosphate-buffered saline (PBS) and then incubated overnight in 5% BSA in PBS containing a rabbit anti-laminin monoclonal antibody diluted 1:100 (Neomarkers, Fremont, CA) and one type-specific MHC primary antibody (type I, BA-F8, 1:50; type IIA, SC-71, 1:10). Following washes in PBS, sections were incubated with secondary antibody (Invitrogen) for 1 hr in the dark at room temperature. Slides were washed and mounted with Vectashield with 4,6-diamidino-2-phenylindole (DAPI). All images were captured and processed on a Leitz DMRBE fluorescent microscope (Leica, Bannockburn, IL) equipped with a MicroMAX digital camera system (Princeton Instruments, Trenton, NJ). Openlab imaging software (Improvision, Waltham, MA) was used for further analysis.

Trichrome staining was performed to determine the extent of fibrosis according to the manufacturer's instructions (Sigma, St. Louis, MO).

Serum CK

Blood samples were collected at euthanasia, allowed to clot for 2 hr at room temperature, then centrifuged at 2,000 *g* for 20 min to isolate serum. Serum was stored at −80°C, and CK was measured later using the assay manufactured by Genzyme (Charlottetown, PEI, Canada).

Magnetic resonance imaging

Three-dimensional (3D)-gradient echo (TR, 19.2 msec; TE, 2.3 msec; flip angle, 30; NEX, 3; slices, 86; slice thickness, 2 mm) and fast spin echo (TR, 2 sec; TE, 16, 32, 48, 64 msec; NEX, 3; slices, 24; slice thickness, 2 mm) axial images of the lower hind limbs were acquired using a 1.5T GE scanner with a wrist volume coil. Each limb was scanned separately. Dogs were induced with a continuous rate of infusion of propofol (1.0–2.0 mg/min/kg) and fentanyl (0.005 mg/kg/min), with maintenance via propofol (0.2 mg/kg/min), fentanyl (0.7 μg/kg/min), and a bolus of cisatracurium (0.1 mg/kg). Respiration, electrocardiogram, O_2 saturation, and blood pressure were monitored.

For analysis, maximal cross-sectional area (CSA_{max}) was measured in the medial (MG) and lateral gastrocnemius (LG), EDL, FDS, and TC of both lower hind limbs using OsiriX software (v.3.8.1). This was performed using the axial images of the 3D-gradient echo sequence and manually tracing the muscles of numerous slices (minimum of six). The CSA_{max} was defined as the average of the largest region of interest (ROI) of a muscle in an axial image and the ROI in the adjacent proximal and distal images, resulting in an average of three slices. As the entire anterior compartment (AC) muscles of the hind limb were acquired within the field of view of the MRI images, we were able to measure muscle volume of this region. The AC consisted of the EDL and TC; however, it became difficult to discern the boundaries of each individual muscle in the distal regions so a global measure of the AC was obtained.

For the T_2 analysis, pixel-by-pixel T_2 maps were generated using OsiriX software (v.3.8.1) in three consecutive slices corresponding to the largest cross-sectional area of the muscles of interest. Therefore, the mean T_2 was the average of the pixels of the three slices in the belly of the muscle. The muscle ROIs for the T_2 analysis were carefully drawn within the borders of the muscle to avoid any potential contamination of intermuscular fascia. In addition to comparing the mean T_2 values of each muscle, we also examined the percentage of pixels above an individualized "threshold" that was defined as three standard deviations below the mean T_2 value of an ROI manually circled in the subcutaneous fat for each time point.

Statistical analysis

Mean values from each experimental group were compared using the two-tailed Student's *t* test or one-way analysis of variance (ANOVA) with Student–Newman–Keuls post hoc analysis, as appropriate. For analysis of MRI data, statistical analyses were performed using SigmaStat software. As there was no difference between the left and right legs in muscle size and T_2 measurements, the two legs were combined into one group. Statistical analyses were performed using repeated-measures one-way ANOVA for the longitudinal measures and two-tailed Student's *t* test for comparisons between the treated and untreated GRMD dogs.

Results

Study design and transgene expression

A total of seven GRMD canines were used in this study that was designed to determine the efficacy of systemic myostatin

inhibition via liver-directed gene transfer of an scAAV8 vector designed to express a secreted dnMSTAT peptide. The AAV8 NAb titer for all canines was <1:20, which was the lower limit of detection for the assay used. The scAAV8-dnMSTAT vector was tested in two normal canines prior to its use in GRMD canines. One normal canine received 10^{12} gc/kg vector via hepatic artery infusion as previously described (Bell *et al.*, 2011), and one normal canine received 10^{12} gc/kg vector via peripheral IV infusion (cephalic vein). Expression levels of dnMSTAT in canine serum are demonstrated up to 20 weeks post injection (Fig. 1A). As expression was similar in canines treated with hepatic artery infusion versus simple, peripheral IV infusion, IV infusion was used as the injection method for the remainder of the study.

Treated GRMD canines received 1.7×10^{12} gc/kg vector ($n=4$) via IV infusion, whereas control dogs received no treatment ($n=3$). Euthanasia occurred 13 months post infusion, at ~23 months of age. Tissue specificity of the liver-specific promoter was confirmed by RT-PCR analysis (Fig. 1B), and serum expression of dnMSTAT was confirmed by western blot (Fig. 1C). Densitometric analysis revealed that serum dnMSTAT levels were approximately two- to threefold of baseline (endogenous myostatin propeptide) (Fig. 1D).

Body weight and muscle weight

Following 13 months of systemic myostatin inhibition, the total body weight of treated GRMD canines was ~25% greater than that of untreated, age-matched controls ($p=0.05$) (Fig. 2A). Individual muscle weights were also larger by the following percentages in treated versus untreated GRMD canines: TC (49%, $p=0.01$), EDL (27%, $p=0.04$), gastrocnemius (43%, $p<0.01$), and FDS (36%, $p=0.05$) (Fig. 2B). There was no significant difference in the ratio of these individual muscle weights to total body weight in treated versus untreated GRMD canines, suggesting that the increased total body weight was largely a result of increased skeletal muscle mass (Fig. 2C).

Muscle fiber-type and -size analysis

Fiber-typing analysis of the EDL and TC muscles was performed. Long-term myostatin inhibition in GRMD canines did not alter the fiber-type composition of either the EDL (Fig. 3A) or TC (Fig. 3B) muscles. However, further analysis revealed that long-term myostatin inhibition resulted in increased fiber size selectively in type IIA fibers by ~20% ($p<0.001$); the size of type I fibers was unaffected by myostatin inhibition (Fig. 3C).

MRI analysis

Representative MRI images are demonstrated in Fig. 4. The CSA_{max} of the MG, LG, FDS, TC, and EDL increased following treatment with liver-targeted systemic myostatin inhibition in the GRMD dogs (Fig. 5A). The CSA_{max} of the lower limb muscles appeared to be either maintained or still growing after 13 months of treatment, at which time the CSA_{max} of the MG, LG, FDS, and TC was significantly greater in treated versus untreated control GRMD canines ($p<0.05$) (Fig. 5B). Correspondingly, the AC volume increased during the year following treatment, with a similar percentage increase (20%) as the CSA_{max} of the TC (18%) and EDL (25%) (Fig. 5C). At 13 months post treatment, the AC

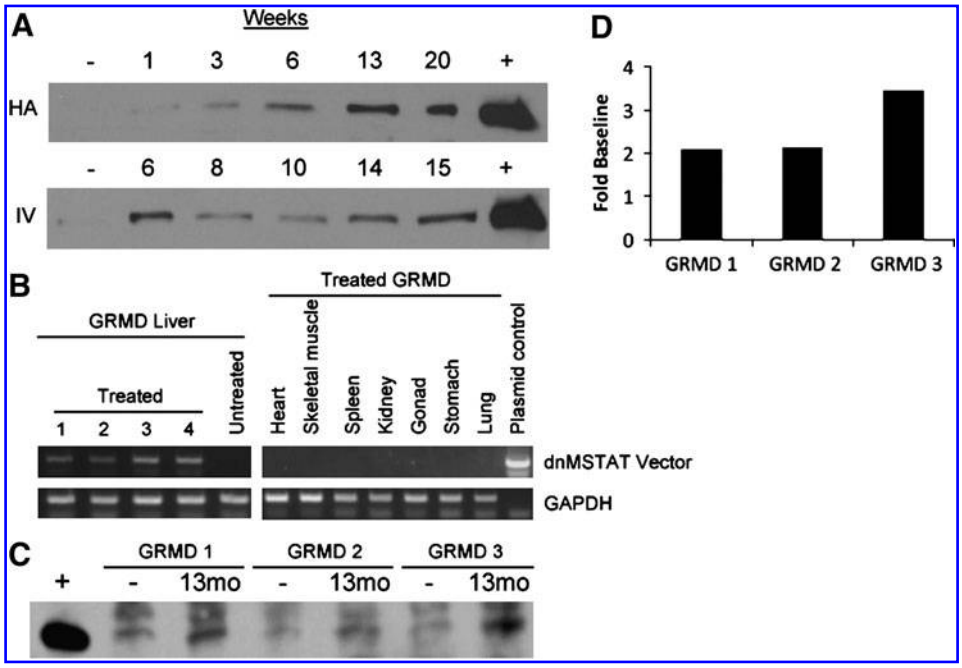

FIG. 1. Expression of dnMSTAT in the canine. **(A)** Two different delivery methods were evaluated in normal canines: hepatic artery (HA) infusion ($n=1$) and IV infusion via a peripheral vein ($n=1$) of 10^{12} gc/kg scAAV8-dnMSTAT with liver-specific promoter. Serum expression of dnMSTAT is demonstrated up to 20 weeks by western blot. Serum collected prior to injection was used as a negative control, and serum collected from a mouse injected with the same vector expressing dnMSTAT was used as a positive control. Expression levels were similar following HA versus IV infusion. **(B)** Liver-specific expression of dnMSTAT is demonstrated via RT-PCR in the GRMD canine ($n=4$) 13 months following IV delivery of 1.7×10^{12} gc/kg scAAV8-dnMSTAT with liver-specific promoter. Representative samples (13 months) from untreated GRMD liver and several organs from treated GRMD canines are shown. **(C)** Serum expression of dnMSTAT in GRMD canines ($n=3$) (one sample was lost due to improper storage) 13 months following IV delivery of 1.7×10^{12} gc/kg scAAV8-dnMSTAT with liver-specific promoter. Serum collected prior to injection was used as a negative control, and serum collected from a mouse injected with the same vector expressing dnMSTAT was used as a positive control. **(D)** Densitometric analysis of the MSTAT band in C.

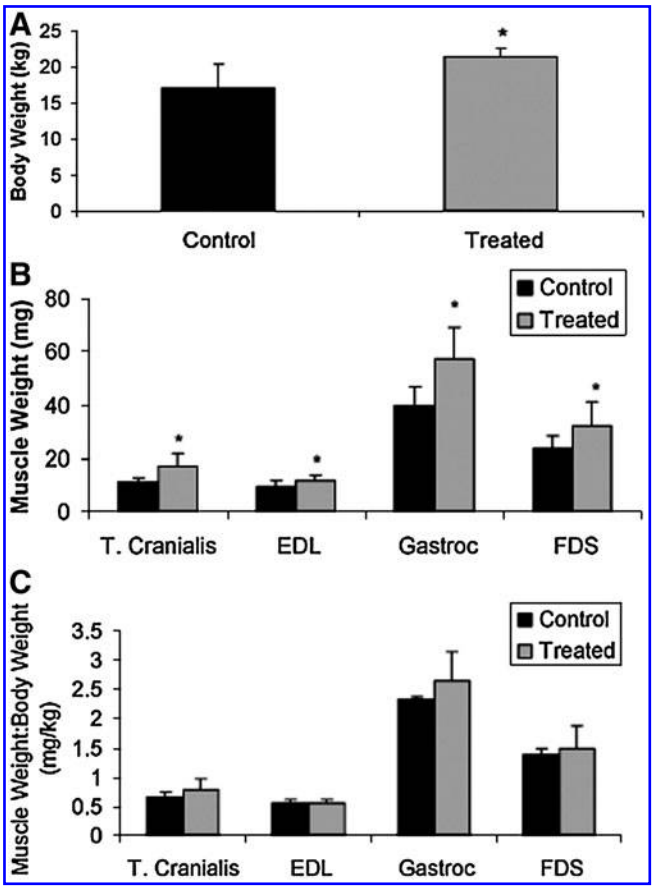

FIG. 2. Effect of myostatin inhibition on body and individual skeletal muscle weight in GRMD canines. **(A)** Total body weight, **(B)** the weights of several individual muscles, and **(C)** the ratio of individual muscle weight to body weight are demonstrated 13 months following injection of 1.7×10^{12} gc/kg scAAV8-dnMSTAT with liver-specific promoter ($n=4$) versus untreated, age-matched GRMD controls ($n=3$). A significant increase in total body weight as well as in the weights of all individual muscles examined was noted. Gastroc, gastrocnemius. *$p<0.05$ vs. control.

volume was significantly greater in treated versus untreated control GRMD canines ($p<0.05$) (Fig. 5D).

The mean T_2 relaxation time of the lower hind-limb muscles was similar in treated versus untreated GRMD canines in the MG, LG, FDS, and EDL, but was significantly lower in the TC of treated versus untreated canines ($p<0.05$) (Fig. 6A). Similarly, the percentage of the muscle region with elevated T_2 pixels was not altered with myostatin inhibition in the MG, LG, FDS, and EDL, but was lower in the TC of treated versus untreated GRMD canines ($p<0.05$) (Fig. 6B). The mean muscle T_2 relaxation time in treated dogs tended to decrease over the 13 months post treatment in the LG ($7\pm4\%$, $p=0.25$), MG ($13\pm2\%$, $p=0.06$), FDS ($10\pm3\%$, $p=0.13$), TC ($6\pm3\%$, $p=0.16$), and EDL ($8\pm2\%$, $p=0.12$).

Serum CK, skeletal muscle fibrosis, and liver pathology

Long-term myostatin inhibition resulted in ~30% reduction in serum CK in treated GRMD canines versus untreated controls ($p<0.05$) (Fig. 7A). In addition, long-term myostatin inhibition resulted in ~20% reduction in fibrosis in the EDL ($p<0.01$) and ~25% reduction in fibrosis in the TC ($p<0.001$) in treated GRMD canines versus untreated controls (Fig. 7B). Representative images are shown in Fig. 7C. Trichrome staining of the liver at 13 months revealed patchy, acellular areas in both treated and untreated GRMD canines (Fig. 8A). These areas did not contain significant collagen content as demonstrated by lack of blue staining. Hematoxylin and eosin (H&E) staining of the liver at 13 months also demonstrated patchy, acellular areas in both treated and untreated GRMD canines (Fig. 8B). No focal areas of mononuclear cell infiltration were noted.

Discussion

This is the first report describing the effects of long-term, systemic myostatin inhibition in a large-animal model of DMD. scAAV8 designed to express a secreted dnMSTAT peptide under the control of a liver-specific promoter was delivered to GRMD canines via simple IV infusion. AAV serotype 8 was used in this study because it was previously demonstrated to be capable of achieving efficient hepatic gene transfer in canines compared with several other serotypes (Bell *et al.*, 2011). The dominant-negative construct that was used to inhibit myostatin in this study is a mutated form of myostatin found in hypermuscular Belgian Blue cattle; it contains an 11-bp deletion that causes a premature stop in the C-terminus, leaving only the inhibitory propeptide to be expressed (Kambadur *et al.*, 1997). In addition, our peptide has been modified to contain a D76A mutation, which makes the inhibitory propeptide resistant to proteolysis (Wolfman *et al.*, 2003). In effect, this construct is a protease-resistant propeptide that can inhibit endogenous myostatin signaling by preventing receptor binding (Lee, 2004). We followed GRMD canines for 13 months following injection of the dnMSTAT construct and found that systemic myostatin inhibition resulted in increased muscle mass in GRMD canines as assessed by MRI and confirmed at tissue harvest. We also found that hypertrophy of type IIA fibers was largely responsible for the increased muscle mass and that reductions in serum CK and muscle fibrosis were associated with long-term myostatin inhibition in GRMD.

Although proof-of-principle studies have demonstrated increased muscle mass following gene transfer of myostatin inhibitors in healthy NHPs (Kota *et al.*, 2009) and canines (Qiao *et al.*, 2009), this is the first report describing myostatin inhibition in a large-animal model of DMD. Similar to what was observed in the healthy NHP (Kota *et al.*, 2009), increased muscle mass secondary to myostatin inhibition in the GRMD canine resulted from selective hypertrophy of type II as opposed to type I fibers. Based on data from mice, the mechanism underlying this selectivity is likely higher expression of the activin IIB receptor (myostatin receptor) in type II fibers (Mendias *et al.*, 2006), although additional investigation will be necessary to confirm this finding in large animals.

We also observed that myostatin inhibition was associated with decreased skeletal muscle fibrosis in GRMD canines at 13 months, a finding that has been previously reported in the *mdx* mouse following myostatin inhibition (Qiao *et al.*, 2008) and genetic ablation of myostatin (Wagner *et al.*, 2002). Evidence suggests that myostatin can regulate skeletal muscle fibrosis by stimulating proliferation of muscle fibroblasts and

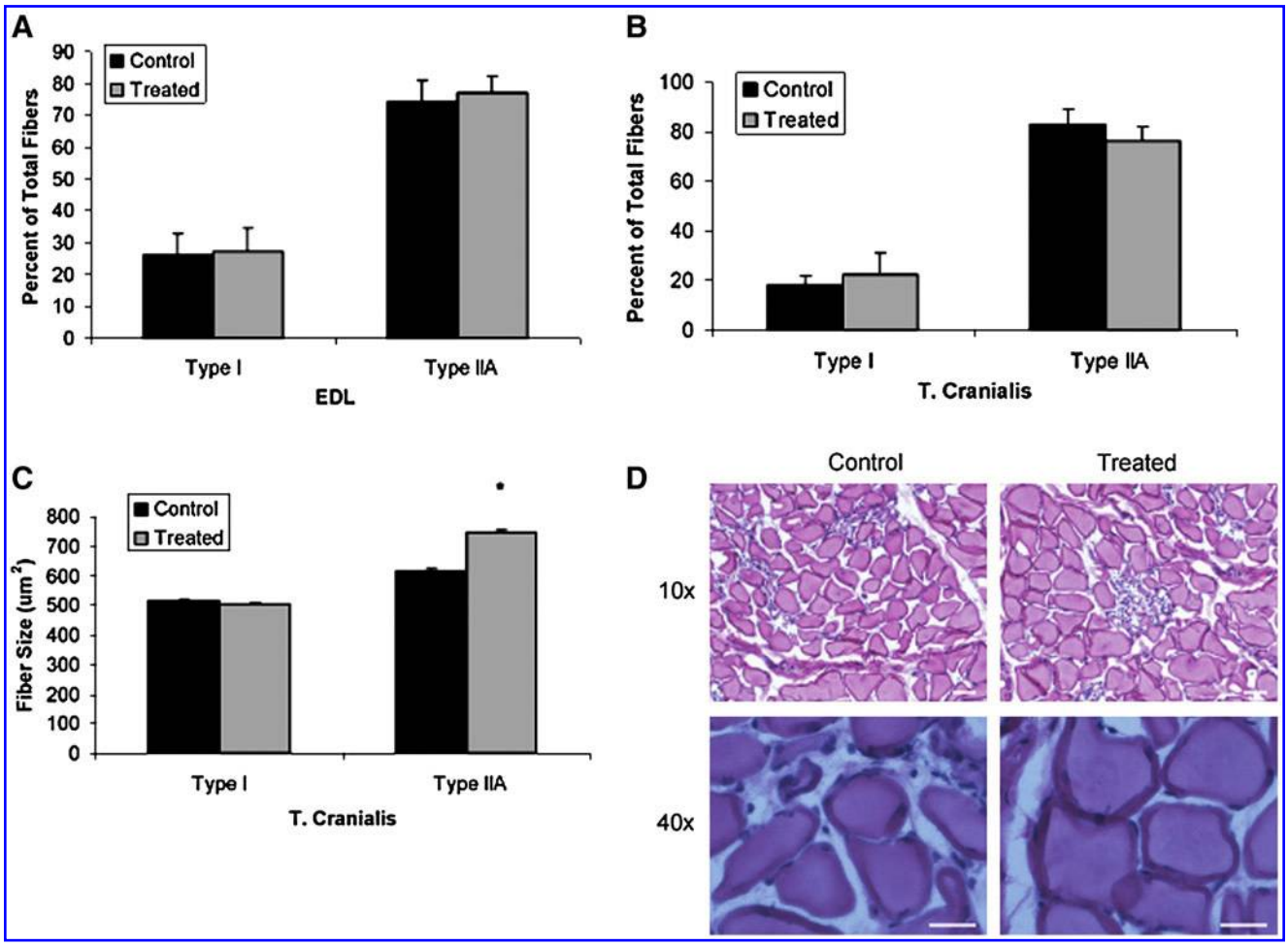

FIG. 3. Effect of myostatin inhibition on skeletal muscle morphology in GRMD canines. MHC fiber-typing analysis of the **(A)** EDL and **(B)** TC is demonstrated 13 months following injection of 1.7×10^{12} gc/kg scAAV8-dnMSTAT with liver-specific promoter ($n = 4$) versus untreated, age-matched GRMD controls ($n = 3$). Myostatin inhibition did not alter the fiber-type composition of the EDL or TC. **(C)** Fiber-size analysis revealed that the increased muscle weight observed in the TC muscle following myostatin inhibition was secondary to hypertrophy of type IIA fibers only. $^*p < 0.05$ vs. control. **(D)** Representative low ($10\times$objective) and high ($40\times$objective) power images of the TC muscle are demonstrated. Scale bars: 200 μm. Color images available online at www.liebertonline.com/hum

expression of extracellular matrix proteins (Li *et al.*, 2008), although this may not be the case in the heart (Cohn *et al.*, 2007). Therefore, myostatin inhibition may attenuate the skeletal muscle phenotype of GRMD canines by at least two independent mechanisms: induction of hypertrophy of type II fibers and blockade of proliferation of muscle fibroblasts.

We also observed reduced serum CK in treated versus untreated GRMD canines, which is indicative of reduced muscle damage. We followed treated GRMD canines in this study with serial MRI. MRI enables sensitive measures of muscle size over time, and magnetic resonance proton transverse relaxation time (T_2) of muscle has been proposed as a marker of disease progression and treatment in dystrophic muscle (Pacak *et al.*, 2007). T_2 is sensitive to a number of characteristics common in dystrophic disease progression, including muscle damage (Foley *et al.*, 1999; Mathur *et al.*,

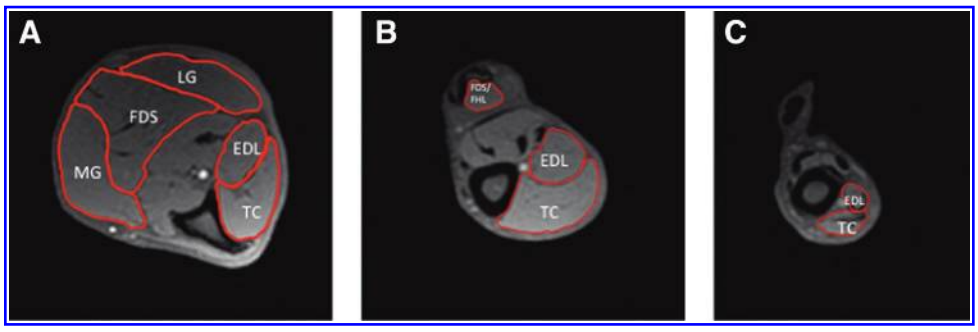

FIG. 4. Representative axial MRI images from GRMD canines. Sample ROIs of **(A)** distal, **(B)** mid, and **(C)** proximal axial slices of the right lower hind limb of a GRMD dog. The AC muscle volume measures were composed of the EDL and TC. Color images available online at www.liebertonline.com/hum

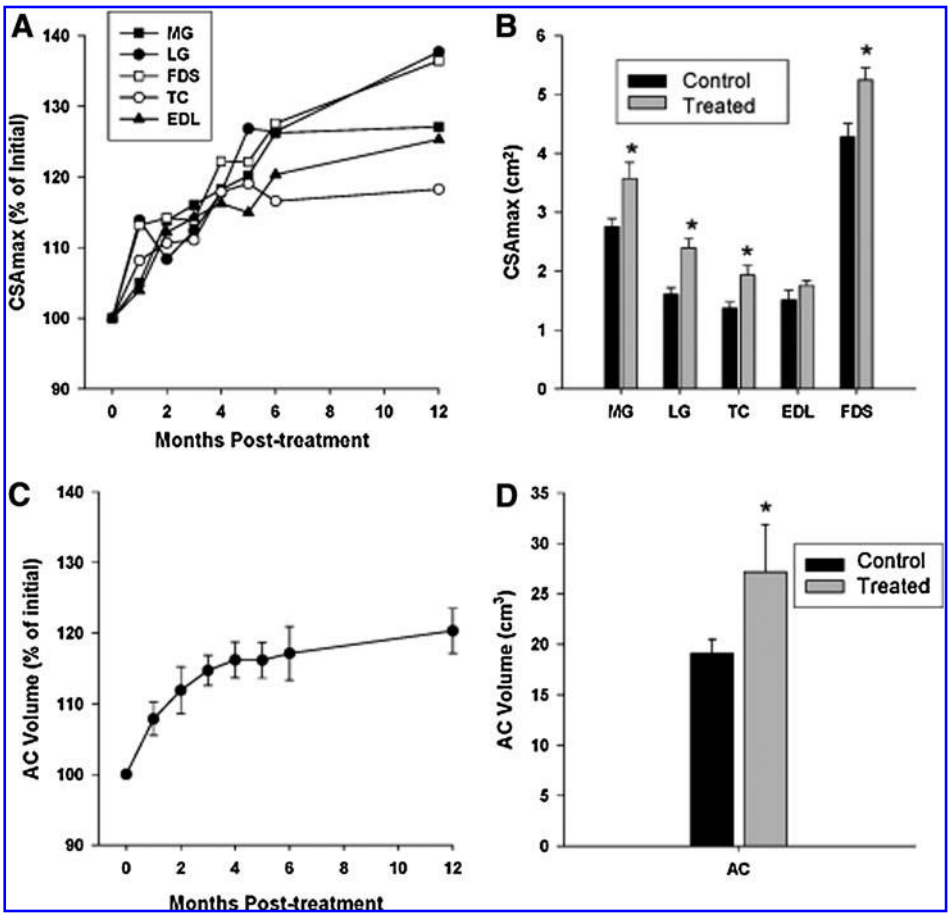

FIG. 5. MRI analysis of muscle morphology in GRMD canines. **(A)** The CSA_{max} of MG, LG, FDS, TC, and EDL at baseline (month 0) and at monthly time points post injection of 1.7×10^{12} gc/kg scAAV8-dnMSTAT with liver-specific promoter for 6 months and at 1 year. Plots represent mean values, with error bars omitted for clarity ($n=4$). **(B)** The CSA_{max} of GRMD canines at 13 months post injection ($n=4$) was compared with untreated, age-matched GRMD controls ($n=3$) (21–25 months of age). $^*p<0.05$ vs. control. **(C)** The AC compartment volume (TC + EDL) of treated GRMD canines was also measured at each time point ($n=4$) and **(D)** compared with age-matched, untreated GRMD controls ($n=3$) at 13 months post injection. $^*p<0.05$ vs. control. Values are means ± SEM.

2011), fatty tissue infiltration (Kan *et al.*, 2009), and fibrosis (Loganathan *et al.*, 2006). Reduced damage and associated edema-like fluid accumulation may have contributed to the lower T_2 in treated versus untreated GRMD canines. Indeed, we observed that muscle T_2 showed a trend to decrease post treatment in all muscles examined, and there was a significant decrease in T_2 in the TC of treated versus untreated animals at the conclusion of the study. Overall, whereas the mean T_2 value reflects a balance between multiple factors, including fibrosis, edema-like fluid accumulation, and fatty-tissue accumulation, the lower T_2 values in the TC of the treated GRMD canines seem most consistent with factors related to reduced susceptibility to injury and the decreased CK levels observed in this study. A rationale for the other muscle groups not demonstrating a significantly lower T_2 is difficult to reconcile, but may be due, in part, to the variability of T_2 values among the canines, the relatively small changes observed, and the small sample size.

We performed this investigation in the GRMD model because it is the largest available animal model of DMD and is considered the gold standard for evaluation of novel therapeutic interventions for DMD (Wang *et al.*, 2009). The phenotype of the GRMD model most closely resembles the human disease with progressive muscle wasting, degeneration and fibrosis, and shortened life span secondary to respiratory failure or cardiomyopathy (Wang *et al.*, 2009). This is in contrast to beagle canine X-linked muscular dystrophy (Shimatsu *et al.*, 2003) and Cavalier King Charles Spaniel models (Walmsley *et al.*, 2010), which are smaller and easier to maintain, but which exhibit a less severe phenotype. In addition, because of the larger size of GRMD canines, the AAV dose and route of administration derived in this model should be translatable to patients with DMD without major up-scaling of vector.

In this study, we evaluated systemic myostatin inhibition via liver-directed gene transfer following a single IV infusion, a strategy we previously employed in the *mdx* mouse using both dnMSTAT (Morine *et al.*, 2010a) and soluble activin IIB receptor (Morine *et al.*, 2010b). Other gene transfer–based approaches to myostatin inhibition previously evaluated in large animals include direct intramuscular injection of vector in healthy NHPs (Kota *et al.*, 2009) and hydrodynamic limb-vein injection of vector in healthy canines (Qiao *et al.*, 2009). Although these investigators observed increased muscle mass in the injected muscles, these local delivery techniques would require multiple injections to target every muscle and muscle group in a DMD patient compared with the single IV infusion performed in our strategy. Furthermore, as myostatin inhibition does not prevent turnover of dystrophin-deficient muscle fibers, transgene expression would be lost over time as repair and regeneration occur (Bartoli *et al.*, 2007; Pacak *et al.*, 2008). This would not be an issue for liver-directed gene transfer in DMD. In addition, our approach takes advantage of the highly efficient synthetic machinery of the liver to secrete the inhibitory peptide into the systemic circulation.

Other investigators have developed systemic myostatin inhibition strategies based on injection of anti-myostatin

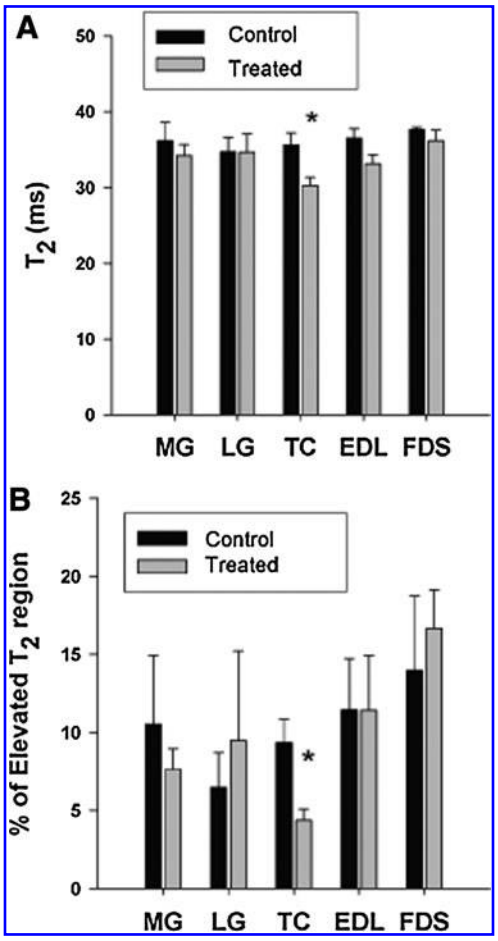

FIG. 6. Analysis of T_2 weighted MRI images in GRMD canines. **(A)** Mean T_2 relaxation time was similar in treated ($n=4$) and untreated ($n=3$) GRMD dogs at 13 months in the MG, LG, EDL, and FDS, whereas T_2 relaxation time was significantly lower in the TC of the treated GRMD dogs compared with untreated, GRMD controls. $^*p<0.05$ vs. control. **(B)** The percentage of elevated pixels was not significantly different at 13 months in treated ($n=4$) versus untreated ($n=3$) dogs in the MG, LG, EDL, and FDS; however, a lower percentage of elevated T_2 values was noted in the TC of treated GRMD dogs versus untreated GRMD controls. $^*p<0.05$ vs. control. Values are means ± SEM.

antibodies (Bogdanovich *et al.*, 2002; Wagner *et al.*, 2008) and soluble activin IIB receptor protein (Pistilli *et al.*, 2011). However, this type of approach would necessitate serial injections based on protein half-life for the duration of a DMD patient's life compared with a single IV infusion with our strategy. In addition, patients would also be at risk for developing NAbs against these injected foreign proteins. In contrast, our dnMSTAT peptide is identical to the endogenous propeptide with the exception of a single-point mutation, and even if the resulting single amino acid substitution has potential for immune activation, evidence suggests that liver production and secretion may induce tolerance to foreign peptides (Mingozzi *et al.*, 2007). Although we did not assay for the presence of NAbs against dnMSTAT that could have resulted in submaximal serum levels of dnMSTAT, we did confirm the presence of serum dnMSTAT at levels approximately two- to threefold above endogenous propeptide levels at 13 months post injection in this study. Further analysis will be necessary to determine the extent, if any, of the humoral response against dnMSTAT following liver-directed gene transfer of AAV8-dnMSTAT in this model.

We also performed pathologic analysis of the livers of treated and untreated GRMD canines at 13 months. We did not observe any increase in fibrosis in treated livers following Trichrome staining, nor did we observe any regions of mononuclear cell infiltration in treated livers following H&E staining. Although this analysis at 13 months does not allow us to rule out an earlier immune response, a recent study did not detect a T-cell response directed against AAV8 capsid following liver-directed gene transfer in canines (Bell *et al.*, 2011). Furthermore, as we confirmed expression of dnMSTAT at 13 months by RT-PCR and western blot, it is unlikely that a significant T-cell response directed against hepatocytes expressing dnMSTAT was mounted at an earlier time point. However, future investigation should be directed at analyzing the T-cell response at an earlier time point following liver-directed gene transfer of AAV8-dnMSTAT in this model to support our preliminary findings.

It should be noted, however, that myostatin inhibition is not a cure for DMD; rather, it is a strategy that can be used to slow the loss of muscle mass characteristic of this disease. Stabilization of DMD would require restoration of dystrophin expression. Several approaches to achieve this are currently being evaluated in clinical trials, including exon skipping (Miyagoe-Suzuki and Takeda, 2010; Moulton and Moulton, 2010; Partridge, 2010), gene transfer of mini-dystrophin (Miyagoe-Suzuki and Takeda, 2010), and nonsense suppression (Finkel, 2010). However, as it is unlikely that any one of these strategies will result in complete dystrophin restoration in every muscle, a combination of myostatin inhibition and dystrophin restoration approaches may provide additional benefit in DMD patients. Furthermore, based on observations in normal mice (Lee *et al.*, 2005; Lee, 2007a), a combination of myostatin inhibition strategies that target other TGF-β family members in addition to myostatin [*i.e.*, follistatin, follistatin-like related gene (FLRG), growth and differentiation factor–associated serum protein-1 (GASP-1), and/or soluble myostatin receptor (Lee, 2004)] may be more effective than a single-agent approach for increasing muscle mass in DMD. However, our prior experiments suggest that this may not be the case in the *mdx* mouse, in which similar benefit was observed with dnMSTAT (Morine *et al.*, 2010a) and the soluble activin IIB receptor (Morine *et al.*, 2010b). Additionally, it is unclear if targeting other TGF-β family members by using the soluble activin IIB receptor or follistatin will result in side effects not observed when targeting myostatin alone with dnMSTAT. Future investigation should be directed at evaluating such combination approaches in GRMD canines.

In summary, this is the first report describing the effects of long-term, systemic myostatin inhibition in a large-animal model of DMD. GRMD canines underwent liver-directed gene transfer of an scAAV8 vector designed to express a secreted dnMSTAT peptide, and we observed increased muscle mass with selective hypertrophy of type IIA fibers in conjunction with reduced serum CK and muscle fibrosis at 13 months. We believe that the safe, simple, and effective nature of our liver-directed gene-transfer strategy makes it an ideal candidate for evaluation as a novel therapeutic

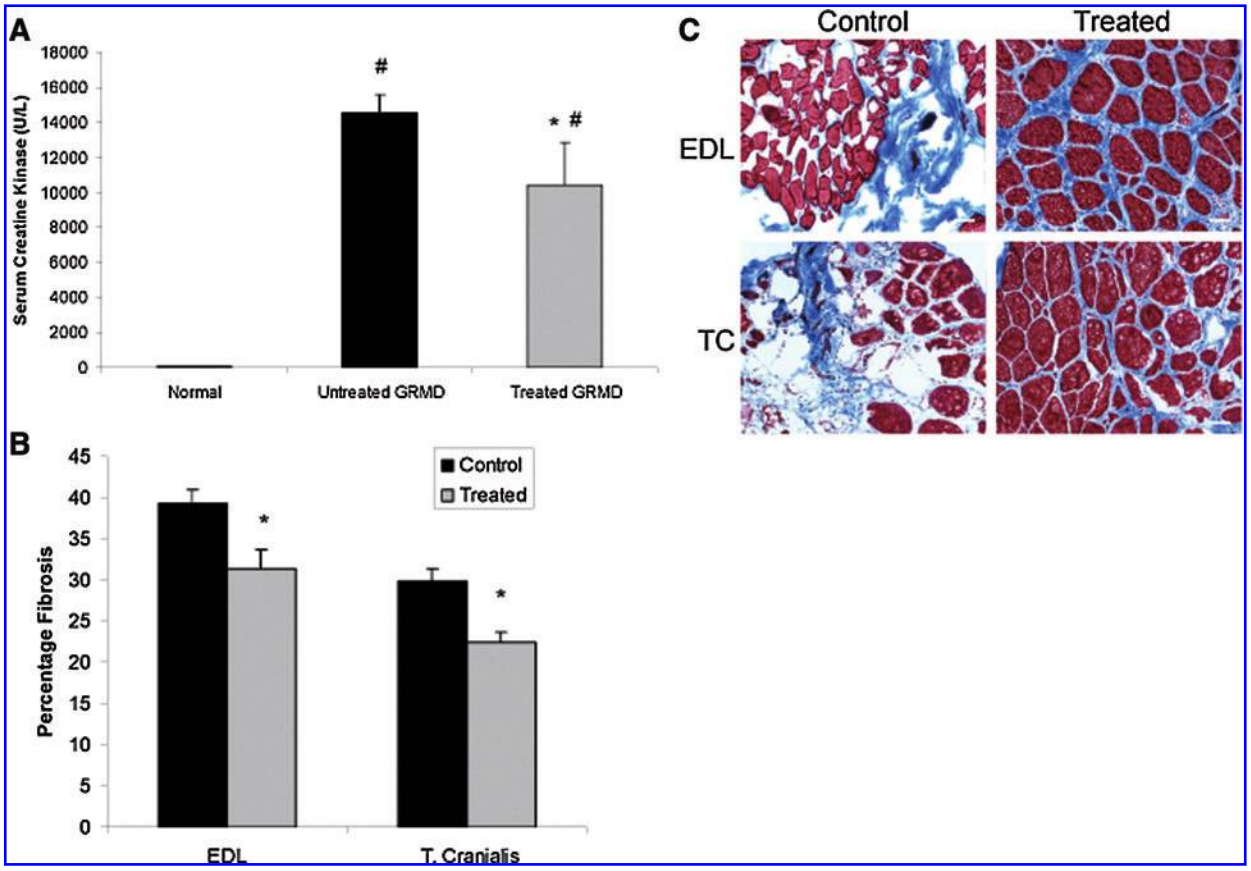

FIG. 7. Effect of myostatin inhibition on serum CK and skeletal muscle fibrosis. **(A)** Serum CK was measured in GRMD canines at 13 months post injection of 1.7×10^{12} gc/kg scAAV8-dnMSTAT with liver-specific promoter ($n = 4$) and compared with age-matched, untreated GRMD canines ($n = 3$). Serum from a healthy, unaffected canine served as a normal control. Serum CK was significantly elevated in both treated and untreated GRMD canines compared with normal, but serum CK was elevated to a lesser extent following myostatin inhibition. #$p < 0.05$ vs. normal; *$p < 0.05$ vs. untreated GRMD. **(B)** The percentage of fibrotic area was quantified following Trichrome staining in the EDL and TC of GRMD canines at 13 months post injection of 1.7×10^{12} gc/kg scAAV8-dnMSTAT with liver-specific promoter ($n = 4$) and compared with age-matched, untreated GRMD canines ($n = 3$). Fibrosis was significantly reduced following myostatin inhibition. *$p < 0.05$ vs. control. **(C)** Representative Trichrome-stained images (10× objective) from the EDL and TC are presented. Scale bars: 200 μm. Color images available online at www.liebertonline.com/hum

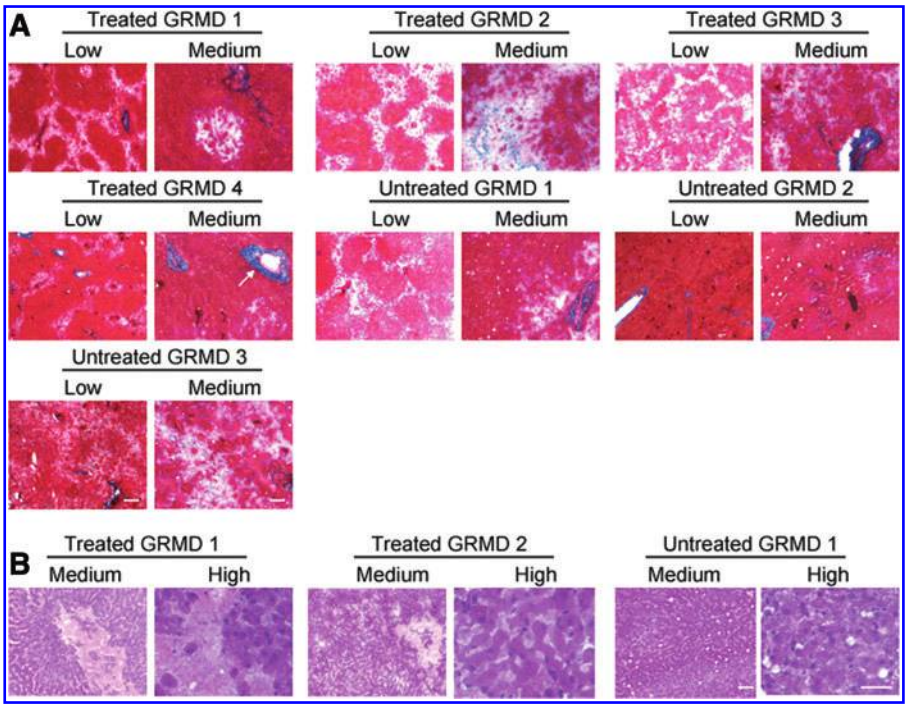

FIG. 8. Liver pathology. **(A)** Trichrome and **(B)** H&E staining were performed on liver samples 13 months post injection of 1.7×10^{12} gc/kg scAAV8-dnMSTAT with liver-specific promoter ($n = 4$) and compared with age-matched, untreated GRMD canines ($n = 3$). Representative images are shown. To reduce redundancy, images from a subset of canines are presented for H&E staining. Low, 2.5× objective; medium, 10× objective; high, 40× objective. Scale bars: 400 μm for low, 200 μm for medium and high. Arrow indicates representative blood vessel (not all blood vessels are labeled). Color images available online at www.liebertonline.com/hum

approach for DMD patients, perhaps in combination with dystrophin-restoration approaches.

Acknowledgments

We thank Mark Haskins (University of Pennsylvania School of Veterinary Medicine, NIH grant RR02512) for support of the animal colony and Derek Wilson and Stephanie Wickham for assistance with imaging analysis. This work was supported by a grant from the NHLBI (P01-HL059407) (to H.L.S.), a grant from the Parent Project Muscular Dystrophy (to H.L.S.), by a Wellstone Muscular Dystrophy Cooperative Center Grant (U54-AR052646) (to H.L.S.), by T32-HL-007748 (to L.T.B.), and by the International Collaborative Effort (ICE) for DMD (to H.L.S.). We thank the Vector Core of the Children's Hospital of Philadelphia and Katherine High, MD, for vector production.

Author Disclosure Statement

No competing financial conflicts exist for L.T.B., M.M.S., S.C.F., K.J.M., C.R., G.E.S., D.T., J.P., J.B., J.N.K., K.V., G.A.W., and H.L.S.

References

Aartsma-Rus, A., Van Deutekom, J.C., Fokkema, I.F., *et al.* (2006). Entries in the Leiden Duchenne muscular dystrophy mutation database: an overview of mutation types and paradoxical cases that confirm the reading-frame rule. Muscle Nerve 34, 135–144.

Bartoli, M., Poupiot, J., Vulin, A., *et al.* (2007). AAV-mediated delivery of a mutated myostatin propeptide ameliorates calpain 3 but not α-sarcoglycan deficiency. Gene Ther. 14, 733–740.

Barton, E.R., Morris, L., Musaro, A., *et al.* (2002). Muscle-specific expression of insulin-like growth factor I counters muscle decline in *mdx* mice. J. Cell Biol. 157, 137–148.

Bell, P., Gao, G., Haskins, M.E., *et al.* (2011). Evaluation of adeno-associated viral vectors for liver-directed gene transfer in dogs. Hum. Gene Ther. [Epub ahead of print].

Bogdanovich, S., Krag, T.O., Barton, E.R., *et al.* (2002). Functional improvement of dystrophic muscle by myostatin blockade. Nature 420, 418–421.

Bogdanovich, S., Perkins, K.J., Krag, T.O., *et al.* (2005). Myostatin propeptide-mediated amelioration of dystrophic pathophysiology. FASEB J. 19, 543–549.

Bogdanovich, S., McNally, E.M., and Khurana, T.S. (2008). Myostatin blockade improves function but not histopathology in a murine model of limb-girdle muscular dystrophy 2C. Muscle Nerve 37, 308–316.

Cohn, R.D., Liang, H.Y., Shetty, R., *et al.* (2007). Myostatin does not regulate cardiac hypertrophy or fibrosis. Neuromuscul. Disord. 17, 290–296.

Denti, M.A., Rosa, A., D'Antona, G., *et al.* (2006). Body-wide gene therapy of Duchenne muscular dystrophy in the *mdx* mouse model. Proc. Natl. Acad. Sci. U.S.A. 103, 3758–3763.

Denti, M.A., Incitti, T., Sthandier, O., *et al.* (2008). Long-term benefit of adeno-associated virus/antisense-mediated exon skipping in dystrophic mice. Hum. Gene Ther. 19, 601–608.

Emery, A.E. (2002). The muscular dystrophies. Lancet 359, 687–695.

Finkel, R.S. (2010). Read-through strategies for suppression of nonsense mutations in Duchenne/Becker muscular dystrophy: aminoglycosides and ataluren (PTC124). J. Child Neurol. 25, 1158–1164.

Foley, J.M., Jayaraman, R.C., Prior, B.M., *et al.* (1999). MR measurements of muscle damage and adaptation after eccentric exercise. J. Appl. Physiol. 87, 2311–2318.

Goyenvalle, A., Vulin, A., Fougerousse, F., *et al.* (2004). Rescue of dystrophic muscle through U7 snRNA-mediated exon skipping. Science 306, 1796–1799.

Gregorevic, P., Blankinship, M.J., Allen, J.M., *et al.* (2004). Systemic delivery of genes to striated muscles using adeno-associated viral vectors. Nat. Med. 10, 828–834.

Harper, S.Q., Hauser, M.A., DelloRusso, C., *et al.* (2002). Modular flexibility of dystrophin: implications for gene therapy of Duchenne muscular dystrophy. Nat. Med. 8, 253–261.

Herzog, R.W., Yang, E.Y., Couto, L.B., *et al.* (1999). Long-term correction of canine hemophilia B by gene transfer of blood coagulation factor IX mediated by adeno-associated viral vector. Nat. Med. 5, 56–63.

Kambadur, R., Sharma, M., Smith, T.P., and Bass, J.J. (1997). Mutations in myostatin (GDF8) in double-muscled Belgian Blue and Piedmontese cattle. Genome Res. 7, 910–916.

Kan, H.E., Scheenen, T.W., Wohlgemuth, M., *et al.* (2009). Quantitative MR imaging of individual muscle involvement in facioscapulohumeral muscular dystrophy. Neuromuscul. Disord. 19, 357–362.

Kornegay, J.N., Li, J., Bogan, J.R., *et al.* (2010). Widespread muscle expression of an AAV9 human mini-dystrophin vector after intravenous injection in neonatal dystrophin-deficient dogs. Mol. Ther. 18, 1501–1508.

Kota, J., Handy, C.R., Haidet, A.M., *et al.* (2009). Follistatin gene delivery enhances muscle growth and strength in nonhuman primates. Sci. Transl. Med. 1, 6ra15.

Lee, S.J. (2004). Regulation of muscle mass by myostatin. Annu. Rev. Cell Dev. Biol. 20, 61–86.

Lee, S.J. (2007a). Quadrupling muscle mass in mice by targeting TGF-β signaling pathways. PLoS One 2, e789.

Lee, S.J. (2007b). Sprinting without myostatin: a genetic determinant of athletic prowess. Trends Genet. 23, 475–477.

Lee, S.J., Reed, L.A., Davies, M.V., *et al.* (2005). Regulation of muscle growth by multiple ligands signaling through activin type II receptors. Proc. Natl. Acad. Sci. U.S.A. 102, 18117–18122.

Li, Z.B., Kollias, H.D., and Wagner, K.R. (2008). Myostatin directly regulates skeletal muscle fibrosis. J. Biol. Chem. 283, 19371–19378.

Liu, M., Yue, Y., Harper, S.Q., *et al.* (2005). Adeno-associated virus-mediated microdystrophin expression protects young mdx muscle from contraction-induced injury. Mol. Ther. 11, 245–256.

Loganathan, R., Bilgen, M., Al-Hafez, B., and Smirnova, I.V. (2006). Characterization of alterations in diabetic myocardial tissue using high resolution MRI. Int. J. Cardiovasc. Imaging 22, 81–90.

Mathur, S., Vohra, R.S., Germain, S.A., *et al.* (2011). Changes in muscle T2 and tissue damage after downhill running in mdx mice. Muscle Nerve 43, 878–886.

McCarty, D.M., Monahan, P.E., and Samulski, R.J. (2001). Self-complementary recombinant adeno-associated virus (scAAV) vectors promote efficient transduction independently of DNA synthesis. Gene Ther. 8, 1248–1254.

McPherron, A.C., Lawler, A.M., and Lee, S.J. (1997). Regulation of skeletal muscle mass in mice by a new TGF-β superfamily member. Nature 387, 83–90.

Mendias, C.L., Marcin, J.E., Calerdon, D.R., and Faulkner, J.A. (2006). Contractile properties of EDL and soleus muscles of myostatin-deficient mice. J. Appl. Physiol. 101, 898–905.

Mingozzi, F., Hasbrouck, N.C., Basner-Tschakarjan, E., *et al.* (2007). Modulation of tolerance to the transgene product in a nonhuman primate model of AAV-mediated gene transfer to liver. Blood 110, 2334–2341.

Miyagoe-Suzuki, Y., and Takeda, S. (2010). Gene therapy for muscle disease. Exp. Cell Res. 316, 3087–3092.

Morine, K.J., Bish, L.T., Pendrak, K., *et al.* (2010a). Systemic myostatin inhibition via liver-targeted gene transfer in normal and dystrophic mice. PLoS One 5, e9176.

Morine, K.J., Bish, L.T., Selsby, J.T., *et al.* (2010b). Activin IIB receptor blockade attenuates dystrophic pathology in a mouse model of Duchenne muscular dystrophy. Muscle Nerve 42, 722–730.

Moulton, H.M., and Moulton, J.D. (2010). Morpholinos and their peptide conjugates: therapeutic promise and challenge for Duchenne muscular dystrophy. Biochim. Biophys. Acta 1798, 2296–2303.

Muntoni, F., Torelli, S., and Ferlini, A. (2003). Dystrophin and mutations: one gene, several proteins, multiple phenotypes. Lancet Neurol. 2, 731–740.

Pacak, C.A., Walter, G.A., Gaidosh, G., *et al.* (2007). Long-term skeletal muscle protection after gene transfer in a mouse model of LGMD-2D. Mol. Ther. 15, 1775–1781.

Pacak, C.A., Conlon, T., Mah, C.S., and Byrne, B.J. (2008). Relative persistence of AAV serotype 1 vector genomes in dystrophic muscle. Genet. Vaccines Ther. 6, 14.

Partridge, T. (2010). The potential of exon skipping for treatment for Duchenne muscular dystrophy. J. Child Neurol. 25, 1165–1170.

Pistilli, E.E., Bogdanovich, S., Goncalves, M.D., *et al.* (2011). Targeting the activin type IIB receptor to improve muscle mass and function in the mdx mouse model of Duchenne muscular dystrophy. Am. J. Pathol. 178, 1287–1297.

Qiao, C., Li, J., Jiang, J., *et al.* (2008). Myostatin propeptide gene delivery by adeno-associated virus serotype 8 vectors enhances muscle growth and ameliorates dystrophic phenotypes in mdx mice. Hum. Gene Ther. 19, 241–254.

Qiao, C., Li, J., Zheng, H., *et al.* (2009). Hydrodynamic limb vein injection of adeno-associated virus serotype 8 vector carrying canine myostatin propeptide gene into normal dogs enhances muscle growth. Hum. Gene Ther. 20, 1–10.

Rodino-Klapac, L.R., Montgomery, C.L., Bremer, W.G., *et al.* (2010). Persistent expression of FLAG-tagged micro dystrophin in nonhuman primates following intramuscular and vascular delivery. Mol. Ther. 18, 109–117.

Schuelke, M., Wagner, K.R., Stolz, L.E., *et al.* (2004). Myostatin mutation associated with gross muscle hypertrophy in a child. N. Engl. J. Med. 350, 2682–2688.

Sharp, N.J., Kornegay, J.N., Van Camp, S.D., *et al.* (1992). An error in dystrophin mRNA processing in golden retriever muscular dystrophy, an animal homologue of Duchenne muscular dystrophy. Genomics 13, 115–121.

Shimatsu, Y., Katagiri, K., Furuta, T., *et al.* (2003). Canine X-linked muscular dystrophy in Japan (CXMDJ). Exp. Anim. 52, 93–97.

Sicinski, P., Geng, Y., Ryder-Cook, A.S., *et al.* (1989). The molecular basis of muscular dystrophy in the mdx mouse: a point mutation. Science 244, 1578–1580.

Tyler, K.L. (2003). Origins and early descriptions of "Duchenne muscular dystrophy." Muscle Nerve 28, 402–422.

Valentine, B.A., Cooper, B.J., de Lahunta, A., *et al.* (1988). Canine X-linked muscular dystrophy. An animal model of Duchenne muscular dystrophy: clinical studies. J. Neurol. Sci. 88, 69–81.

Wagner, K.R., McPherron, A.C., Winik, N., and Lee, S.J. (2002). Loss of myostatin attenuates severity of muscular dystrophy in mdx mice. Ann. Neurol. 52, 832–836.

Wagner, K.R., Fleckenstein, J.L., Amato, A.A., *et al.* (2008). A phase I/II trial of MYO-029 in adult subjects with muscular dystrophy. Ann. Neurol. 63, 561–571.

Walmsley, G.L., Arechavala-Gomeza, V., Fernandez-Fuente, M., *et al.* (2010). A Duchenne muscular dystrophy gene hot spot mutation in dystrophin-deficient Cavalier King Charles Spaniels is amenable to exon 51 skipping. PLoS One 5, e8647.

Wang, Z., Kuhr, C.S., Allen, J.M., *et al.* (2007). Sustained AAV-mediated dystrophin expression in a canine model of Duchenne muscular dystrophy with a brief course of immunosuppression. Mol. Ther. 15, 1160–1166.

Wang, Z., Chamberlain, J.S., Tapscott, S.J., and Storb, R. (2009). Gene therapy in large animal models of muscular dystrophy. ILAR J. 50, 187–198.

Wolfman, N.M., McPherron, A.C., Pappano, W.N., *et al.* (2003). Activation of latent myostatin by the BMP-1/tolloid family of metalloproteinases. Proc. Natl. Acad. Sci. U.S.A. 100, 15842–15846.

Yokota, T., Lu, Q.L., Partridge, T., *et al.* (2009). Efficacy of systemic morpholino exon-skipping in Duchenne dystrophy dogs. Ann. Neurol. 65, 667–676.

Address correspondence to:
Dr. Lawrence T. Bish
B400 Richards Building
3700 Hamilton Walk
Philadelphia, PA 19104

E-mail: bish@mail.med.upenn.edu

Received for publication June 13, 2011;
accepted after revision July 25, 2011.

Published online: July 25, 2011.

This article has been cited by:

1. Michele A Scully, Shree Pandya, Richard T Moxley. 2013. Review of Phase II and Phase III clinical trials for Duchenne muscular dystrophy. *Expert Opinion on Orphan Drugs* **1**:1, 33-46. [CrossRef]
2. Michele A Scully, Shree Pandya, Richard T Moxley. 2013. Review of Phase II and Phase III clinical trials for Duchenne muscular dystrophy. *Expert Opinion on Orphan Drugs* **1**:1, 33-46. [CrossRef]
3. Zhonghai Yan, Hao Yan, Hailong Ou. 2012. Human thyroxine binding globulin (TBG) promoter directs efficient and sustaining transgene expression in liver-specific pattern. *Gene* **506**:2, 289-294. [CrossRef]